

Topological superfluid responses of superconducting Dirac semimetals

Jun-Ang Wang^{1,2,*}, Mohamed Assili^{1,†} and Panagiotis Kotetes^{1,‡}

¹CAS Key Laboratory of Theoretical Physics, *Institute of Theoretical Physics, Chinese Academy of Sciences, Beijing 100190, China*

²School of Physical Sciences, *University of Chinese Academy of Sciences, Beijing 100049, China*

 (Received 1 December 2022; revised 8 November 2023; accepted 18 May 2024; published 6 June 2024)

We demonstrate that topological constraints do not only dictate the geometric part of the superfluid stiffness, but can also govern the *total* superfluid stiffness. By introducing a general adiabatic approach for superfluid responses, we showcase such a possibility by proving that the stiffness of a superconducting Dirac cone in two dimensions (2D) is proportional to its topological charge. By relying on the emergent Lorentz invariance of Dirac electrons, we unify the superfluid stiffness and quantum capacitance in these systems. Based on this connection, we further predict a topological origin for the quantum capacitance of a Josephson junction where 2D massless Dirac electrons are sandwiched between two conventional superconductors. We show that the topological responses persist upon effecting strain, are resilient against weak disorder, and can be experimentally controlled via a Zeeman field. Remarkably, the nonuniversal topological quantization of the two superfluid responses, yet implies the universal topological quantization of the admittance modulus of the superconducting Dirac system in units of conductance. The quantum admittance effect arises when embedding the superconducting Dirac system in an ac electrical circuit with a frequency tuned at the absorption edge. These findings are in principle experimentally observable in graphene-superconductor hybrids.

DOI: [10.1103/PhysRevResearch.6.L022053](https://doi.org/10.1103/PhysRevResearch.6.L022053)

The exploration of the interplay between topology and quantum geometry through superfluid responses of time-reversal invariant superconductors (SCs) [1] is currently in the spotlight [2–7]. Such a pursuit got substantially boosted after experiments in magic angle twisted bilayer graphene (MATBG) provided evidences for a nonvanishing superfluid stiffness despite the almost flat energy dispersion which governs transport [8,9]. This quite unusual result was subsequently understood in terms of lower bounds set by topological invariants dictating the MATBG band structure [10–15]. These bounds impose constraints on the so-called geometric contribution to the stiffness, which becomes relevant when superconductivity is harbored by flat bands. However, no topological constraints have been so far predicted for the *total* superfluid stiffness. The potential discovery of systems whose total stiffness is equal or proportional to a topological invariant promises to deepen our understanding of topological platforms and set the stage for novel applications.

In this Letter, we show that topological constraints dictate the total superfluid stiffness of superconducting Dirac semimetals (SDSs). Notably, a quantized total superfluid stiffness has already been theoretically predicted for

superconducting graphene [16–19], which constitutes a prototypical SDS in its Dirac regime [20]. However, the quantization itself, along with its topological origin and resulting implications have not yet been discussed. After Refs. [16–19], the superfluid stiffness of a superconducting Dirac cone (D_{cone}) reads at charge neutrality as

$$D_{\text{cone}} = \Delta/\pi, \quad (1)$$

and becomes quantized in units of $\Delta \geq 0$, which is the intrinsic or proximity-induced conventional pairing gap felt by graphene [21–27]. In the above, we set the reduced Planck constant \hbar and the electric charge unit e to unity.

This quantization is rather puzzling as it cannot be explained by topological bounds of the type predicted for MATBG since, here, the dispersions are strongly non flat, and D_{cone} receives equal contributions from both interband (geometric) and intraband (conventional) parts [4].

In this work, we resolve this conundrum by proving that $\pi D_{\text{cone}}/\Delta$ is a topological invariant. This result is a consequence of nontrivial topology for a single Dirac cone in the presence of a phase which twists its mass, similar to the Jackiw-Rossi model [28]. As we further explain in our companion work [29], the quantization is also a manifestation of one-dimensional chiral anomaly [30,31]. These properties, along with the arising Lorentz invariance, also render the quantum capacitance c_Q of a Josephson junction sandwiching a Dirac cone topological and equal to

$$c_{Q,\text{cone}} = D_{\text{cone}}/v_D^2, \quad (2)$$

where v_D is the group velocity of the Dirac dispersion.

Both effects enjoy topological robustness as long as the chiral symmetry of the Dirac Hamiltonian is preserved. To

*wangjunang@itp.ac.cn

†m.assili@itp.ac.cn

‡kotetes@itp.ac.cn

Published by the American Physical Society under the terms of the [Creative Commons Attribution 4.0 International license](https://creativecommons.org/licenses/by/4.0/). Further distribution of this work must maintain attribution to the author(s) and the published article's title, journal citation, and DOI.

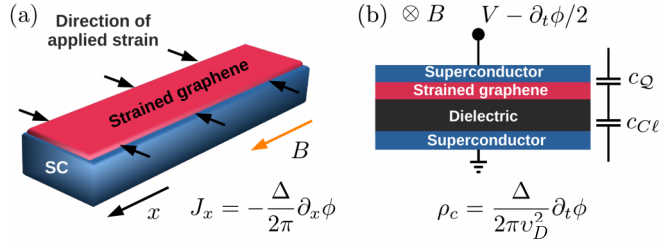


FIG. 1. Hybrids of strained graphene and superconductors (SCs). Each graphene Dirac cone leads to a quantized superfluid stiffness $D = -J_x/(\partial_x \phi/2) = \Delta/\pi$ and quantum capacitance $c_Q = \rho/(\partial_t \phi/2) = \Delta/\pi v_D^2$. A graphene cone sees a pairing gap Δ and Fermi velocity v_D . The quantized Dirac contributions can be disentangled by tuning strain, a Zeeman energy B , and/or the classical capacitance of the junction c_{cl} .

back this claim, we show that Eqs. (1) and (2) persist upon adding nonuniform strain which leads to an energy spectrum that consists of relativistic pseudo-Landau levels (pLLs) [32–39]. We show that for the pLL flat bands, D and c_Q are purely of a geometric origin, and are solely carried by the zeroth pseudo-Landau levels (OpLLs). Hence, we reveal that the topological quantization dictating the total superfluid stiffness of the SDS, further imposes the quantization for the geometric part of the stiffness when the Dirac bands flatten due to strain.

We propose to experimentally detect these SDS effects in superconducting (un)strained graphene hybrids, such as the ones shown in Fig. 1. The quantized contribution of the Dirac electrons can be disentangled by applying a magnetic field which couples to graphene electrons only through a Zeeman energy scale B . The Zeeman energy sets the occupancy of the energy levels of the SC. Hence, by manipulating its strength $|B|$, one is in a position to controllably add or subtract the contribution of the Dirac part of the band structure. Most importantly, we bring forward that, at charge neutrality, the smoking gun signature of the topological effects predicted here is the observation of the universal topological quantization of the admittance modulus Y_{mod} of the SDS, when it is embedded in an ac electrical circuit. Specifically, when the ac frequency ω is tuned at the absorption edge 2Δ , Y_{mod} equals the number of Dirac cones in units of conductance.

We commence our analysis by unifying the superfluid stiffness tensor elements D_{ij} and the Josephson quantum capacitance (JQC) c_Q in SDSs. The former quantities define the coefficients which link the charge current $\mathbf{J}(\mathbf{r})$ to the spatially dependent gauge invariant vector potential $\mathbf{A}(\mathbf{r}) + \nabla\phi(\mathbf{r})/2$, where $\mathbf{A}(\mathbf{r})$ denotes the electromagnetic vector potential and $\phi(\mathbf{r})$ is the superconducting phase. Therefore, we have the defining relation:

$$J_i(\mathbf{r}) = -D_{ij}[A_j(\mathbf{r}) + \partial_j\phi(\mathbf{r})/2], \quad (3)$$

where $i, j = x, y$ for a two-dimensional system. The JQC can be defined in an analogous fashion, through the excess charge density $\rho_c(t)$ induced in a Josephson junction due to the presence of the gauge invariant voltage $V(t) - \partial_t\phi(t)/2$. For a two-terminal Josephson junction as in Fig. 1(b), $V(t)$ and $\phi(t)$ define the voltage and phase biases imposed across the junction. Therefore, we define c_Q as the response

coefficient which satisfies the relation:

$$\rho_c(t) = -c_Q[V(t) - \partial_t\phi(t)/2]. \quad (4)$$

The apparent similarities between Eqs. (3) and (4) imply that the charge and current responses can be unified by here introducing the relativistic three-current given as $J_\mu = D_{\mu\nu}(A^\nu - \partial^\nu\phi/2)$ with $\mu, \nu = 0, 1, 2$, metric tensor $\text{diag}\{1, -1, -1\}$, and $D_{00} = -c_Q$. Hence, the superfluid stiffness and the JQC are proportional in systems with an emergent Lorentz invariance. As a result, for superconducting massless Dirac electrons with a “speed of light” v_D , Lorentz invariance leads to the constraint $D_{xx,yy} = v_D^2 c_Q$, which indeed holds for Eq. (2). Having settled the connection between D and c_Q in SDSs, we now proceed by examining how nontrivial topology further imposes their nonuniversal quantization.

Our starting point is the Hamiltonian for a generic two-dimensional time-reversal invariant SC:

$$\hat{H}(\mathbf{p}) = \hat{h}(\mathbf{p})\tau_3 + \Delta\tau_1, \quad (5)$$

where $\tau_{1,2,3}$ denote Pauli matrices which are defined in Nambu space. The latter is spanned by electrons with spin up and momentum \mathbf{p} , and, their time-reversed hole partners with spin down and momentum $-\mathbf{p}$. From Eqs. (3) and (4) we infer that $D_{\mu\nu}$ can be identified with the coefficients relating the uniform current J_μ induced by a nonzero spatiotemporally uniform phase gradient $\partial_\mu\phi$. In particular, to obtain expressions for the superfluid stiffness tensor elements D_{ij} , we consider small deviations of the superconducting phase away from the value $\phi = 0$, i.e., $\phi(\mathbf{r}) \approx (\partial_x\phi)x + (\partial_y\phi)y$, with $\partial_{x,y}\phi$ being constants. Subsequently, we phase twist the pairing term according to $\Delta\tau_1 \mapsto \Delta\tau_1 e^{-i\phi(\mathbf{r})\tau_3}$ and determine the spatially uniform current component J_i within linear response to the phase gradient $\partial_j\phi$. In the same spirit, D_{00} is found using linear response theory to a linearlyvarying time-dependent phase of the form $\phi(t) \approx (\partial_t\phi)t$.

By adopting this alternative approach, in Ref. [29] we show that $D_{\mu\nu}$ can be expressed as suitable response coefficients of the respective adiabatic Hamiltonian:

$$\hat{\mathcal{H}}(\mathbf{p}, \phi) = \hat{h}(\mathbf{p})\tau_3 + \Delta\tau_1 e^{-i\phi\tau_3}, \quad (6)$$

where the superconducting phase ϕ is now viewed as an additional synthetic momentum. Using the above adiabatic Hamiltonian, Ref. [29] provides concrete expressions for the elements $D_{\mu\nu}$. Specifically, for D_{ij} we find [29]:

$$D_{ij} = 2 \int dP \text{Tr}[\hat{v}_i(\mathbf{p}) \mathbb{1}_\tau \hat{\mathcal{F}}_{P_j\phi}(\epsilon, \mathbf{p}, \phi)], \quad (7)$$

where “Tr” denotes trace over all internal degrees of freedom. For compactness, we employed the shorthand notation $\int dP \equiv \int_{\text{BZ}} \frac{d\mathbf{p}}{(2\pi)^2} \int_{-\infty}^{+\infty} \frac{d\epsilon}{2\pi}$, with $\epsilon \in (-\infty, +\infty)$ corresponding to the frequency in imaginary time. The momenta are generally defined in a two-dimensional Brillouin zone (BZ), since the SC is considered to be a crystalline material. When evaluating the superfluid stiffness carried by a Dirac cone, we replace the BZ by \mathbb{R}^2 [29].

In Eq. (7), we also introduced the group velocity $\hat{v}(\mathbf{p}) = \partial_{\mathbf{p}}\hat{h}(\mathbf{p})$ of the normal phase Hamiltonian $\hat{h}(\mathbf{p})$, along with the

adiabatic matrix Green function:

$$\hat{\mathcal{G}}^{-1}(\epsilon, \mathbf{p}, \phi) = i\epsilon + B - \hat{\mathcal{H}}(\mathbf{p}, \phi). \quad (8)$$

We note once again that the Zeeman energy B sets the Bogoliubov-Fermi level. The last ingredient of the adiabatic approach is the matrix Berry curvature function:

$$\hat{\mathcal{F}}_{p_j\phi} = 1/2(\partial_\epsilon \hat{\mathcal{G}}^{-1})\hat{\mathcal{G}}(\partial_\phi \hat{\mathcal{G}}^{-1})\hat{\mathcal{G}}(\partial_{p_j} \hat{\mathcal{G}}^{-1})\hat{\mathcal{G}} - \partial_\phi \leftrightarrow \partial_{p_j}, \quad (9)$$

where we suppressed the arguments of the Green functions for notational convenience. In spite of the fact that our adiabatic approach is fully equivalent to the standard method of evaluating the superfluid stiffness, it is unique in uncovering the possible underlying topological properties of the system, since it is already expressed in the terms of a curvature function in a synthetic space [29].

We now proceed by recovering the result of Ref. [16] shown in Eq. (1), and proving that $\pi D_{\text{cone}}/\Delta$ is a topological invariant. At charge neutrality, the chemical potential μ is set to be zero and the normal phase Hamiltonian for a given graphene valley $\lambda = \pm 1$ reads as [20]

$$\hat{h}_\lambda(\mathbf{p}) = v_D(p_x\sigma_1 + \lambda p_y\sigma_2), \quad (10)$$

where $\sigma_{1,2,3}$ denote Pauli matrices acting in the sublattice space spanned by the two interpenetrating triangular lattices of graphene [20]. Note that, for graphene, electrons couple to holes of different valleys [40]. Nonetheless, by a suitable choice of basis, each valley of graphene is described by a Hamiltonian of the form shown in Eq. (5).

The adiabatic Hamiltonian obtained for the $\lambda = +1$ valley of the graphene model in Eq. (10) takes the form

$$\hat{\mathcal{H}}_{\text{cone}}(\mathbf{p}, \phi) = v_D(p_x\sigma_1 + p_y\sigma_2)\tau_3 + \Delta\mathbb{1}_\sigma\tau_1e^{-i\phi\tau_3}. \quad (11)$$

Notably, the operator $\hat{\Pi} = \sigma_3\tau_3$ establishes a chiral symmetry $\{\hat{\mathcal{H}}_{\text{cone}}(\mathbf{p}, \phi), \hat{\Pi}\} = \hat{0}$. Its presence guarantees that there exists a basis in which $\hat{\Pi} = \mathbb{1}_\sigma\tau_3$ and the adiabatic Hamiltonian becomes block-off diagonal according to $\hat{\mathcal{H}}_{\text{cone}}(\mathbf{p}, \phi) = \hat{A}(\mathbf{p}, \phi)\tau_+ + \hat{A}^\dagger(\mathbf{p}, \phi)\tau_-$ [41]. Here, we introduced the off-diagonal matrices $\tau_\pm = (\tau_1 \pm i\tau_2)/2$, along with the upper off-diagonal Hamiltonian block:

$$\hat{A}(\mathbf{p}, \phi) = (-v_D p_x, -v_D p_y, \Delta \cos \phi) \cdot \boldsymbol{\sigma} + i\Delta \sin \phi \mathbb{1}_\sigma. \quad (12)$$

The topological properties of the adiabatic Hamiltonian are encoded in the topological invariant $w_3 \in \mathbb{Z}$ [41]. This coincides with the winding number of $\hat{A}(\mathbf{p}, \phi)$. We now write $w_3 = \int_0^{2\pi} d\phi w_3(\phi)/2\pi$, where we defined the winding number densities $w_3(\phi) = \int d\mathbf{p} w_3(\mathbf{p}, \phi)/2\pi$ and

$$w_3(\mathbf{p}, \phi) = \text{tr}[(\hat{A}\partial_{p_x}\hat{A}^{-1})(\hat{A}\partial_{p_y}\hat{A}^{-1})(\hat{A}\partial_\phi\hat{A}^{-1})]. \quad (13)$$

Notably, in the case of Dirac systems, $w_3(\mathbf{p}, \phi)$ and $w_3(\phi)$ are independent of ϕ . Consequently, besides w_3 , also $w_3(\phi)$ is quantized. In particular, for a phase twist of 2π we have $w_3(\phi) = w_3$. The behaviors of $w_3(\mathbf{p}, \phi)$ and $w_3(\phi)$ become relevant here since, for $B = 0$, we find [29]:

$$D_{\text{cone}} = - \int \frac{d\mathbf{p}}{(2\pi)^2} E(\mathbf{p}) w_3(\mathbf{p}, \phi), \quad (14)$$

where $E(\mathbf{p}) = \sqrt{(v_D\mathbf{p})^2 + \Delta^2}$ and we made use of the fact that $D_{xx,yy} = D_{\text{cone}}$ and $D_{xy,xy} = 0$.

The above result highlights that the outcome for the superfluid stiffness is determined by the topological properties of the adiabatic Dirac Hamiltonian. In fact, we are now in a position to prove that $\pi D_{\text{cone}}/\Delta$ is a topological invariant itself. For this purpose, we note that for the evaluation of $w_3(\mathbf{p}, \phi)$ we can linearize \hat{A} with respect to ϕ according to $\hat{A}(\mathbf{p}, \phi) \simeq \mathbf{g}(\mathbf{p}) \cdot \boldsymbol{\sigma} + i\Delta\phi\mathbb{1}_\sigma$. Here, we defined the vector $\mathbf{g}(\mathbf{p}) = (-v_D p_x, -v_D p_y, \Delta)$, where $|\mathbf{g}(\mathbf{p})| = E(\mathbf{p})$. Under these assumptions, we find

$$\frac{D_{\text{cone}}}{\Delta/\pi} = \int \frac{d\mathbf{p}}{4\pi i} E(\mathbf{p}) \text{tr}\{\hat{A}_0^{-1}(\mathbf{p})[\partial_{p_x}\hat{A}_0(\mathbf{p})][\partial_{p_y}\hat{A}_0^{-1}(\mathbf{p})]\}, \quad (15)$$

where we took into account that ϕ can be set to zero after ∂_ϕ is carried out. In the above, we introduced $\hat{A}_0(\mathbf{p}) \equiv \hat{A}(\mathbf{p}, \phi = 0) = \mathbf{g}(\mathbf{p}) \cdot \boldsymbol{\sigma}$ which is a hermitian matrix with $\hat{A}_0^{-1}(\mathbf{p}) = \hat{A}_0(\mathbf{p})/|\mathbf{g}(\mathbf{p})|^2$. The antisymmetry of the integrand under the exchange $p_x \leftrightarrow p_y$ further allows us to obtain the expression

$$\frac{D_{\text{cone}}}{\Delta/\pi} = 2 \int \frac{d\mathbf{p}}{4\pi} \hat{\mathbf{g}}(\mathbf{p}) \cdot [\partial_{p_x}\hat{\mathbf{g}}(\mathbf{p}) \times \partial_{p_y}\hat{\mathbf{g}}(\mathbf{p})], \quad (16)$$

with the unit vector $\hat{\mathbf{g}}(\mathbf{p}) = \mathbf{g}(\mathbf{p})/|\mathbf{g}(\mathbf{p})|$. When the momentum space is compact, the above integral yields an integer, that coincides with the first Chern number of the negative eigenstate of $\hat{A}_0(\mathbf{p})$. However, due to the Dirac nature of the adiabatic Hamiltonian, the integral yields $1/2$ [42]. Hence, the quantization of the superfluid stiffness directly probes the presence of a Weyl point at the origin of the synthetic coordinate space (p_x, p_y, Δ) , since it is exactly there where $\hat{A}_0(\mathbf{p})$ and $|\mathbf{g}(\mathbf{p})|$ become zero.

The origin of the nontrivial topology can be traced back to the properties of the Hamiltonian in the absence of a phase bias: $\hat{H}_{\text{cone}}(\mathbf{p}) = v_D(p_x\sigma_1 + p_y\sigma_2)\tau_3 + \Delta\mathbb{1}_\sigma\tau_1$. This Hamiltonian features two chiral symmetries effected by the operators $\hat{\Pi} = \sigma_3\tau_3$ and $\hat{\Pi}' = \tau_2$, which lead to a unitary symmetry with the generating operator $\hat{\mathcal{O}} = \sigma_3\tau_1$. Employing the unitary transformation $(\hat{\Pi} + \tau_1)/\sqrt{2}$ block diagonalizes the unitary symmetry operator according to $\hat{\mathcal{O}}_\tau = \tau\mathbb{1}_\sigma$ and the Hamiltonian into the blocks $\hat{H}_\tau(\mathbf{p}) = \tau\mathbf{g}(\mathbf{p}) \cdot \boldsymbol{\sigma}$. Since the occupied bands of the two massive Dirac Hamiltonians yield opposite fractional first Chern numbers with values $\tau/2$, we conclude that the superfluid stiffness is proportional to the difference of these two first Chern numbers. The latter can be viewed as a fractional ‘‘spin’’ [43] or dipole [29] first Chern number.

It is important to examine the robustness of the quantized value of the superfluid stiffness against external perturbations. We first investigate situations which preserve chiral symmetry, as for instance the introduction of disorder in the pairing gap and the application of strain. The impact of weak and uncorrelated spatial disorder in the pairing gap is analyzed in our Supplemental Material [44] within the first-order Born approximation [45]. We find that the quantization persists, but in the disordered case Δ is replaced by its spatially averaged value.

We now consider the presence of strain which varies linearly in space. This scenario is particularly interesting, since the low-energy description of strained graphene solely consists of pLLs which possess a perfectly flat dispersion, therefore allowing us to make connections with topological

constraints associated with quantum geometry. We adopt a strain profile which conserves the p_y momentum and yields the Hamiltonian [20,34,38,44]:

$$\hat{h}_\lambda^B(p_y) = \omega_B \left[\frac{\ell_B}{\sqrt{2}} \hat{p}_x \sigma_1 + \frac{1}{\sqrt{2} \ell_B} (x + \lambda p_y \ell_B^2) \sigma_2 \right], \quad (17)$$

where $\omega_B = \sqrt{2} v_D / \ell_B$. Here, ℓ_B denotes the pseudomagnetic length. Each valley supports a single 0pLL which, for the given choice of strain profile, is an eigenstate of σ_3 with eigenvalue -1 . The remaining spectrum of $\hat{h}_\lambda^B(p_y)$ consists of two families of non-zero-energy pLLs, with eigenenergies $\varepsilon_{\sigma,n}(p_y) = \sigma \varepsilon_n(p_y) = \sigma \omega_B \sqrt{n}$ for $n \geq 1$. Each pLL sees a degeneracy per area which is equal to $1/2\pi \ell_B^2$ for a single valley and a single spin projection [20].

Since the energy dispersions are flat, it is more convenient to deduce the contribution of each pLL to the stiffness using the standard expression for the interband part D_{inter} [5]. In the following we restrict to the $\lambda = +1$ valley and denote the corresponding pLL eigenvectors as $|u_\alpha(p_y)\rangle$, where $\alpha = (\sigma, n)$ compactly labels the two quantum numbers. As we show in Ref. [44], D_{inter} can be expressed as a sum of contributions defined per level α :

$$D_{\text{inter}}^\alpha = \frac{\Delta}{\pi} \int \frac{dp_y}{W} \langle \partial_{p_y} u_\alpha(p_y) | \hat{M}_\alpha(p_y) | \partial_{p_y} u_\alpha(p_y) \rangle P_\alpha(p_y), \quad (18)$$

where W is the width of the sample. Here, $E_\alpha(p_y) = \sqrt{\varepsilon_\alpha^2(p_y) + \Delta^2}$, while $P_\alpha(p_y) = \Theta[E_\alpha(p_y) - |B|]$ controls the occupation of each level, where Θ is the Heaviside step function. The operator $\hat{M}_\alpha(p_y)$ is defined as follows:

$$\hat{M}_\alpha(p_y) = \frac{2\Delta}{E_\alpha(p_y)} \frac{\hat{h}_{\lambda=+1}^B(p_y) - \varepsilon_\alpha(p_y)}{\hat{h}_{\lambda=+1}^B(p_y) + \varepsilon_\alpha(p_y)}. \quad (19)$$

Equation (18) holds as long as $\hat{h}_\lambda^B(p_y) + \varepsilon_\alpha(p_y)$ for all pLLs, which is exactly the case here as we explain in Ref. [44].

By employing Eq. (18) at charge neutrality and $B = 0$, we confirm that now only the 0pLLs contribute to the stiffness, which is still given by Eq. (1). However, the stiffness is now purely geometric. To show this, we use that $\hat{M}_{0\text{pLL}}(p_y) = 2(\hat{1} - |u_{0\text{pLL}}(p_y)\rangle\langle u_{0\text{pLL}}(p_y)|)$. This allows us to express the stiffness in terms of the quantum metric of the 0pLL, i.e., $g_{0\text{pLL}}(p_y) = \langle \partial_{p_y} u_{0\text{pLL}}(p_y) | (\hat{1} - |u_{0\text{pLL}}(p_y)\rangle\langle u_{0\text{pLL}}(p_y)|) | \partial_{p_y} u_{0\text{pLL}}(p_y) \rangle = \ell_B^2/2$. The result of Eq. (1) is recovered by evaluating the integral $\int dp_y/W$ by accounting for the degeneracy of the pLLs.

The arising robustness of the superfluid stiffness for weak strains is indeed expected as long as the Dirac points in (\mathbf{p}, ϕ) space of the adiabatic Hamiltonian persist. This holds when the pLL degeneracy is much smaller than unity, since then, the Dirac point is not removed but only ‘‘moves’’ in synthetic space. As a matter of fact, our adiabatic approach is still valid for weak strains and we can re-evaluate Eq. (14) for $p_y \mapsto p_y + \lambda x / \ell_B^2$ and $x \mapsto \phi / \partial_x \phi$. We find that corrections to Eq. (1) become negligible as long as $\omega_B \ll \Delta$ and ℓ_B is sufficiently smaller than the sample’s width W for a strip geometry.

So far we have focused on an ideal (un)strained Dirac cone. However, in realistic experiments the nonconical part in graphene’s band structure also contributes and spoils the

universal behavior. Nonetheless, it is still possible to isolate the quantized part by introducing an inplane Zeeman field, which can selectively modify the occupation of the various states. In Fig. 2 we present numerical results for the superfluid stiffness of strained armchair graphene nanoribbons (GNRs) at charge neutrality and varying B . Notably, when B crosses the energy bands, the arising Bogoliubov-Fermi points lead to an additional contribution to the intraband part of the superfluid stiffness, with the latter being obtained using the formula [44]:

$$D_{\text{intra}} = -\frac{\Delta}{\pi} \int \frac{dp_y}{W} \sum_\alpha \frac{\Delta [\partial_{p_y} \varepsilon_\alpha(p_y)]^2}{2E_\alpha(p_y)} \frac{d}{dE_\alpha(p_y)} \frac{P_\alpha(p_y)}{E_\alpha(p_y)}. \quad (20)$$

The results of Fig. 2 verify that fields $|B| > \Delta$ enable the experimental detection of the quantized contribution of the 0pLLs. In Fig. 2(d) we confirm the quantized jump of the total stiffness across $|B| = \Delta$, where any deviation from the expected quantization is only due to numerical finite-size effects. Our analysis reveals that, armchair GNRs are better-suited for observing the quantized jump compared to zigzag GNRs. This is because zigzag GNRs harbor additional edge flat bands which appear even without strain [20] and spoil the quantization [44].

Another aspect that remains to be addressed concerns the impact of detuning away from charge neutrality due to a nonzero chemical potential μ which leads to $\varepsilon_{0\text{pLL}}^{\mu \neq 0}(p_y) = -\mu$ and $\varepsilon_{\sigma,n}^{\mu \neq 0}(p_y) = \sigma \omega_B \sqrt{n} - \mu$ for $n \geq 1$ and $\sigma = \pm 1$. Now, all pLLs contribute to the stiffness. Specifically, the contribution of the 0pLLs now becomes

$$D_{\lambda,0\text{pLL}}^{\mu \neq 0} = \frac{\Delta}{\pi} \frac{1}{\sqrt{1 + (\mu/\Delta)^2}} \frac{1}{1 - (\frac{\mu}{\omega_B/2})^2}. \quad (21)$$

Besides a renormalized Δ , an additional factor emerges which diverges for $|\mu| = \omega_B/2$. Thus, the stiffness can be strongly enhanced by tuning the system to this resonance. In fact, such resonances appear for all pLLs [44].

After investigating the superfluid stiffness, we now evaluate the quantum capacitance [46–51] for a Josephson junction fabricated by contacting an ideal strained monolayer graphene hybrid [52–60] to a conventional SC, as shown in Fig. 1(b). Using the model in Eq. (17) for strained graphene, we find that the two-valley JQC at charge neutrality and $B = 0$ takes the exact form [44]:

$$c_Q^{B=\mu=0} = 2 \cdot \frac{\Delta}{\pi v_D^2} \left\{ \left(\frac{\Delta}{2\omega_B} \right) \zeta[3/2, (\Delta/\omega_B)^2] - \left(\frac{\omega_B}{2\Delta} \right)^2 \right\} \quad (22)$$

with the Hurwitz zeta function ζ . Thus, at charge neutrality, weak strains $\omega_B \ll \Delta$ yield $c_Q \rightarrow 2 \cdot \Delta / (\pi v_D^2) \equiv c_0$. This result marks the topological regime and is in accordance with the value set by the emergent Lorentz invariance. In contrast, for $\omega_B \gg \Delta$ only the 0pLLs contribute with $c_Q/c_0 \rightarrow (\omega_B/2\Delta)^2 \gg 1$. For $\Delta = 0.2$ meV and $v_D = 10^6$ m/s, we find $c_0 \simeq 5$ nF/cm². Therefore, tailoring the classical capacitance of the junction c_{cl} , so that $c_{cl} \gg c_Q$, in principle, enables the detection of the underlying

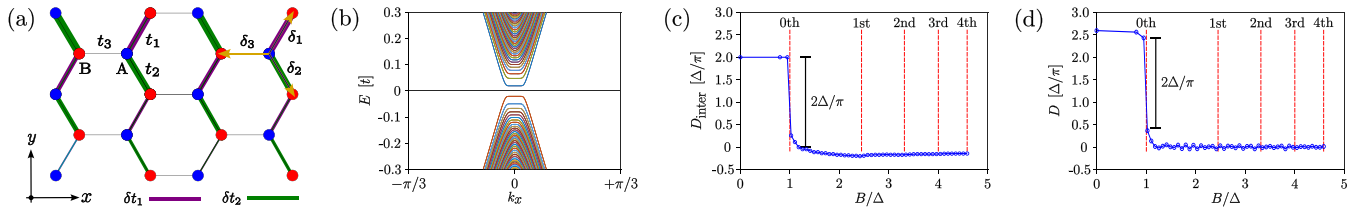


FIG. 2. (a) Schematic illustration of the model adopted for an armchair graphene nanoribbon (GNR). We consider nonuniform strain which renders the x component of the pseudo-vector potential nonzero and increasing with increasing y , as indicated by the thickness of the green and purple lines. (b) Electronic band structure of (a) as a function of the conserved wave number k_x . First, we numerically obtain the spectrum for an armchair graphene GNR of width $W = 601 \times \sqrt{3}a_0$, where a_0 is the carbon-carbon distance, and $\omega_B \simeq 0.045$. Subsequently, we add a conventional superconducting gap $\Delta = 0.02$. pLLs emerge in the interval $-W/2\ell_B^2 \leq k_x \leq +W/2\ell_B^2$ of the first Brillouin zone where a_0 is set to unity for convenience. (c) and (d) show numerical results for the interband and total superfluid stiffness components as functions of an inplane Zeeman field B for the same values discussed in (b). The dashed vertical red lines indicate the energies for the pLLs in the presence of the nonzero Δ . From (c) we verify that $D_{\text{inter}} \approx \frac{2\Delta}{\pi}$ for $B = 0$. Across $B/\Delta = 1$, the total superfluid stiffness drops by approximately $2\Delta/\pi$ as shown in (d). All energies are expressed in units of t , i.e., the nearest-neighbor hopping in the absence of strain. Finally, for the numerics we have replaced the delta function entering in Eq. (20) by a Lorentzian with width $\Gamma = 0.001$.

properties of the Dirac points. This may be possible by observing Coulomb-blockade-induced charging effects, which can be controlled by means of strain [44] and Zeeman field [29] engineering.

We conclude by discussing broader implications of the topological quantization of D and c_Q demonstrated here. First of all, the invariance of the two response coefficients for weak strains implies that flat band SCs which are dictated by a solely geometric quantized stiffness, can be adiabatically mapped to SDSs and the arising quantization linked to the quantum metric can be understood via topological constraints on the total SDS superfluid stiffness. Even more, based on the observation that moiré twisting can be effectively viewed as the application of strain [61], we infer that the nonstandard topological properties proposed here for strained SDSs can be also applicable to their moiré-twisted counterparts.

In this spirit, we expect that the geometric superfluid stiffness of MATBG [10–15] can be possibly attributed to the topological superfluid stiffness of untwisted bilayer graphene. Although we leave the verification of the above conjecture for a future work [62], we here stress that such a scenario is indeed plausible because the total superfluid stiffness of a number of s uncoupled graphene layers, or more general of a number of s uncoupled Dirac cones, satisfies the quantization law $D^{(s)} = |s|D_{\text{cone}}$ [29]. Therefore, the here-proposed connection between Dirac cones and flat band systems opens the door to predicting and linking distinct quantum materials and devices which yet share the same topological superfluid responses.

Aside from the above concept, the nonuniversal topological quantization for $D^{(s)}$ further implies the *universal* quantization

of the admittance modulus Y_{mod} of the SDS for $\omega = 2\Delta$, i.e., at the absorption edge. This relies on the fact that for $0 < \omega \leq 2\Delta$ and at zero temperature, a fully gapped nondisordered SC behaves as a perfect inductor, with $Y_{\text{mod}} = D/\omega$ [63]. Thus, in our case we find

$$Y_{\text{mod}}^{(s)}(\mu = 0, 0 < \omega \leq 2\Delta) = |s| \frac{e^2}{h} \frac{2\Delta}{\hbar\omega}, \quad (23)$$

where the quantum of conductance e^2/h appeared after restoring e and \hbar . From the above, we confirm that a quantum admittance effect (QAE) emerges for $\hbar\omega = 2\Delta$.

Currently, however, it is challenging to experimentally observe the above QAE in graphene-SC hybrids, since the chemical potential can be only reduced down to ~ 1 meV [64]. This sets existing platforms in the antipodal regime $|\mu| \gg \Delta$, thus, raising the question of how does the stiffness and the admittance behave in this limit. Re-evaluating the stiffness for $\mu \neq 0$ yields that a higher-order Dirac cone with vorticity s carries a stiffness $D^{(s)}(|\mu| \gg \Delta) \approx |s||\mu|/2\pi$ [44]. In fact, for such a higher-order SDS, the stiffness is proportional to $|s|$ for all μ [29]. Since a gate potential V_g modifies μ according to $\mu + V_g$, we propose to experimentally measure $dD^{(s)}/dV_g \approx |s|/2\pi$ which, while it is not a topological invariant, it is still approximately universally quantized.

We are grateful to M. Cuoco, M. T. Mercaldo, T. Shi, and H.-Q. Xu for helpful discussions. We acknowledge funding from the National Natural Science Foundation of China (Grant No. 12074392).

- [1] J. R. Schrieffer, *Theory of Superconductivity* (Benjamin, New York, 1964).
- [2] S. Peotta and P. Törmä, Superfluidity in topologically nontrivial flat bands, *Nat. Commun.* **6**, 8944 (2015).
- [3] A. Julku, S. Peotta, T. I. Vanhala, D.-H. Kim, and P. Törmä, Geometric origin of superfluidity in the Lieb-lattice flat band, *Phys. Rev. Lett.* **117**, 045303 (2016).

- [4] L. Liang, T. I. Vanhala, S. Peotta, T. Siro, A. Harju, and P. Törmä, Band geometry, Berry curvature, and superfluid weight, *Phys. Rev. B* **95**, 024515 (2017).
- [5] P. Törmä, S. Peotta, and B. A. Bernevig, Superfluidity and quantum geometry in twisted multilayer systems, *Nat. Rev. Phys.* **4**, 528 (2022).

- [6] E. Rossi, Quantum metric and correlated states in two-dimensional systems, *Curr. Opin. Solid State Mater. Sci.* **25**, 100952 (2021).
- [7] J. Herzog-Arbeitman, A. Chew, K.-E. Huhtinen, P. Törmä, and B. A. Bernevig, Many-body superconductivity in topological flat bands, [arXiv:2209.00007](https://arxiv.org/abs/2209.00007) (2022).
- [8] Y. Cao, V. Fatemi, S. Fang, K. Watanabe, T. Taniguchi, E. Kaxiras, and P. Jarillo-Herrero, Unconventional superconductivity in magic-angle graphene superlattices, *Nature (London)* **556**, 43 (2018).
- [9] M. Yankowitz, S. Chen, H. Polshyn, Y. Zhang, K. Watanabe, T. Taniguchi, D. Graf, A. F. Young, and C. R. Dean, Tuning superconductivity in twisted bilayer graphene, *Science* **363**, 1059 (2019).
- [10] J. Ahn, S. Park, and B.-J. Yang, Failure of Nielsen-Ninomiya theorem and fragile topology in two-dimensional systems with space-time inversion symmetry: Application to twisted bilayer graphene at magic angle, *Phys. Rev. X* **9**, 021013 (2019).
- [11] T. Hazra, N. Verma, and M. Randeria, Bounds on the superconducting transition temperature: Applications to twisted bilayer graphene and cold atoms, *Phys. Rev. X* **9**, 031049 (2019).
- [12] X. Hu, T. Hyart, D. I. Pikulin, and E. Rossi, Geometric and conventional contribution to the superfluid weight in twisted bilayer graphene, *Phys. Rev. Lett.* **123**, 237002 (2019).
- [13] A. Julku, T. J. Peltonen, L. Liang, T. T. Heikkilä, and P. Törmä, Superfluid weight and Berezinskii-Kosterlitz-Thouless transition temperature of twisted bilayer graphene, *Phys. Rev. B* **101**, 060505 (2020).
- [14] F. Xie, Z. Song, B. Lian, and B. A. Bernevig, Topology-bounded superfluid weight in twisted bilayer graphene, *Phys. Rev. Lett.* **124**, 167002 (2020).
- [15] J. Herzog-Arbeitman, V. Peri, F. Schindler, S. D. Huber, and B. A. Bernevig, Superfluid weight bounds from symmetry and quantum geometry in flat bands, *Phys. Rev. Lett.* **128**, 087002 (2022).
- [16] N. B. Kopnin and E. B. Sonin, BCS superconductivity of Dirac electrons in graphene layers, *Phys. Rev. Lett.* **100**, 246808 (2008); B. Uchoa and A. H. Castro Neto, Comment on BCS superconductivity of Dirac electrons in graphene layers, *ibid.* **102**, 109701 (2009); N. B. Kopnin and E. B. Sonin, Kopnin and sonin reply, *ibid.* **102**, 109702 (2009).
- [17] N. B. Kopnin and E. B. Sonin, Supercurrent in superconducting graphene, *Phys. Rev. B* **82**, 014516 (2010).
- [18] N. B. Kopnin, Surface superconductivity in multilayered rhombohedral graphene: Supercurrent, *JETP Lett.* **94**, 81 (2011).
- [19] T. J. Peltonen and T. T. Heikkilä, Flat-band superconductivity in periodically strained graphene: Mean-field and Berezinskii-Kosterlitz-Thouless transition, *J. Phys.: Condens. Matter* **32**, 365603 (2020).
- [20] A. H. Castro Neto, F. Guinea, N. M. R. Peres, K. S. Novoselov, and A. K. Geim, The electronic properties of graphene, *Rev. Mod. Phys.* **81**, 109 (2009).
- [21] B. Uchoa and K. Seo, Superconducting states for semi-Dirac fermions at zero and finite magnetic fields, *Phys. Rev. B* **96**, 220503(R) (2017).
- [22] L. Brey and H. A. Fertig, Electronic states of graphene nanoribbons studied with the Dirac equation, *Phys. Rev. B* **73**, 235411 (2006).
- [23] K. Wakabayashi, K. Sasaki, T. Nakanishi, and T. Enoki, Electronic states of graphene nanoribbons and analytical solutions, *Sci. Technol. Adv. Mater.* **11**, 054504 (2010).
- [24] L. Covaci and F. M. Peeters, Superconducting proximity effect in graphene under inhomogeneous strain, *Phys. Rev. B* **84**, 241401(R) (2011).
- [25] B. Uchoa and Y. Barlas, Superconducting states in Pseudo-Landau-levels of strained graphene, *Phys. Rev. Lett.* **111**, 046604 (2013).
- [26] B. Roy and V. Juričić, Strain-induced time-reversal odd superconductivity in graphene, *Phys. Rev. B* **90**, 041413(R) (2014).
- [27] V. J. Kauppila, F. Aikebaier, and T. T. Heikkilä, Flat-band superconductivity in strained Dirac materials, *Phys. Rev. B* **93**, 214505 (2016).
- [28] R. Jackiw and P. Rossi, Zero modes of the vortex-fermion system, *Nucl. Phys. B* **190**, 681 (1981).
- [29] J.-A. Wang, M. Assili, and P. Kotetes, companion paper, Superfluid stiffness and Josephson quantum capacitance: Adiabatic approach and topological effects, *Phys. Rev. Res.* **6**, 023256 (2024).
- [30] A. J. Niemi and G. W. Semenoff, Axial-anomaly-induced fermion fractionization and effective Gauge-theory actions in odd-dimensional space-times, *Phys. Rev. Lett.* **51**, 2077 (1983).
- [31] S. Weinberg, *The Quantum Theory of Fields* (Cambridge University Press, New York, USA, 1996).
- [32] M. Neek-Amal, L. Covaci, and F. M. Peeters, Nanoengineered nonuniform strain in graphene using nanopillars, *Phys. Rev. B* **86**, 041405(R) (2012).
- [33] M. Neek-Amal and F. M. Peeters, Graphene on hexagonal lattice substrate: Stress and pseudo-magnetic field, *Appl. Phys. Lett.* **104**, 173106 (2014).
- [34] G. Salerno, T. Ozawa, H. M. Price, and I. Carusotto, How to directly observe Landau levels in driven-dissipative strained honeycomb lattices, *2D Mater.* **2**, 034015 (2015).
- [35] Y. Fan, T. Iwashita, and T. Egami, Programmable extreme pseudomagnetic fields in graphene by a uniaxial stretch, *Phys. Rev. Lett.* **115**, 045501 (2015).
- [36] P. Nigge, A. C. Qu, É. L. Hurtubise, E. Mårzell, S. Link, G. Tom, M. Zonno, M. Michiardi, M. Schneider, S. Zhdanovich, G. Levy, U. Starke, C. Gutiérrez, D. Bonn, S. A. Burke, M. Franz, A. Damascelli, Room temperature strain-induced Landau levels in graphene on a wafer-scale platform, *Sci. Adv.* **5**, eaaw5593 (2019).
- [37] C.-C. Hsu, M. L. Teague, J.-Q. Wang, and N.-C. Yeh, Nanoscale strain engineering of giant pseudo-magnetic fields, valley polarization, and topological channels in graphene, *Sci. Adv.* **6**, eaat9488 (2020).
- [38] M. Jamotte, N. Goldman, and M. D. Liberto, Strain and pseudo-magnetic fields in optical lattices from density-assisted tunneling, *Commun. Phys.* **5**, 30 (2022).
- [39] T. Liu and H. Z. Lu, Analytic solution to pseudo-Landau levels in strongly bent graphene nanoribbons, *Phys. Rev. Res.* **4**, 023137 (2022).
- [40] C. W. J. Beenakker, Specular Andreev reflection in graphene, *Phys. Rev. Lett.* **97**, 067007 (2006).
- [41] A. P. Schnyder, S. Ryu, A. Furusaki, and A. W. W. Ludwig, Classification of topological insulators and superconductors in three spatial dimensions, *Phys. Rev. B* **78**, 195125 (2008).
- [42] G. E. Volovik, *The Universe in a Helium Droplet* (Oxford University Press, New York, 2003).

- [43] D. N. Sheng, Z. Y. Weng, L. Sheng, and F. D. M. Haldane, Quantum spin-Hall effect and topologically invariant chern numbers, *Phys. Rev. Lett.* **97**, 036808 (2006).
- [44] See Supplemental Material at <http://link.aps.org/supplemental/10.1103/PhysRevResearch.6.L022053> for additional technical details on: (a) the effects of weak uncorrelated disorder on the quantization of the superfluid stiffness, (b) the model employed for the study of strained graphene, (c) and (d) analytical/numerical calculations for the superfluid stiffness of strained graphene hybrids, and (e) the evaluation of the Josephson quantum capacitance. It contains Refs. [17,29,45].
- [45] A. A. Zyuzin and P. Simon, Disorder-induced exceptional points and nodal lines in Dirac superconductors, *Phys. Rev. B* **99**, 165145 (2019).
- [46] J. Fernández-Rossier, J. J. Palacios, and L. Brey, Electronic structure of gated graphene and graphene ribbons, *Phys. Rev. B* **75**, 205441 (2007).
- [47] J. Guo, Y. Yoon, and Y. Ouyang, Gate electrostatics and quantum capacitance of graphene nanoribbons, *Nano Lett.* **7**, 1935 (2007).
- [48] T. Fang, A. Konar, H. Xing, and D. Jena, Carrier statistics and quantum capacitance of graphene sheets and ribbons, *Appl. Phys. Lett.* **91**, 092109 (2007).
- [49] J. Xia, F. Chen, J. Li, and N. Tao, Measurement of the quantum capacitance of graphene, *Nat. Nanotechnol.* **4**, 505 (2009).
- [50] S. Dröscher, P. Roulleau, F. Molitor, P. Studerus, C. Stampfer, T. Ihn, K. Ensslin, Quantum capacitance and density of states of graphene, *Appl. Phys. Lett.* **96**, 152104 (2010).
- [51] L. A. Ponomarenko, R. Yang, R. V. Gorbachev, P. Blake, A. S. Mayorov, K. S. Novoselov, M. I. Katsnelson, and A. K. Geim, Density of states and zero Landau level probed through capacitance of graphene, *Phys. Rev. Lett.* **105**, 136801 (2010).
- [52] H. B. Heersche, P. Jarillo-Herrero, J. B. Oostinga, L. M. K. Vandersypen, and A. F. Morpurgo, Bipolar supercurrent in graphene, *Nature (London)* **446**, 56 (2007).
- [53] X. Du, I. Skachko, A. Barker, and E. Y. Andrei, Approaching ballistic transport in suspended graphene, *Nat. Nanotechnol.* **3**, 491 (2008).
- [54] J.-H. Choi, G.-H. Lee, S. Park, D. Jeong, J.-O Lee, H.-S. Sim, Y.-J. Doh, and H.-J. Lee, Complete gate control of supercurrent in graphene p-n junctions, *Nat. Commun.* **4**, 2525 (2013).
- [55] N. Mizuno, B. Nielsen, and X. Du, Ballistic-like supercurrent in suspended graphene Josephson weak links, *Nat. Commun.* **4**, 2716 (2013).
- [56] V. E. Calado, S. Goswami, G. Nanda, M. Diez, A. R. Akhmerov, K. Watanabe, T. Taniguchi, T. M. Klapwijk, and L. M. K. Vandersypen, Ballistic Josephson junctions in edge-contacted graphene, *Nat. Nanotechnol.* **10**, 761 (2015).
- [57] F. Amet, C. T. Ke, I. V. Borzenets, Y.-M. Wang, K. Watanabe, T. Taniguchi, R. S. Deacon, M. Yamamoto, Y. Bomze, S. Tarucha, and G. Finkelstein, Supercurrent in the quantum Hall regime, *Science* **352**, 966 (2016).
- [58] M. Ben Shalom, M. J. Zhu, V. I. Fal'ko, A. Mishchenko, A. V. Kretinin, K. S. Novoselov, C. R. Woods, K. Watanabe, T. Taniguchi, A. K. Geim, and J. R. Prance, Quantum oscillations of the critical current and high-field superconducting proximity in ballistic graphene, *Nat. Phys.* **12**, 318 (2016).
- [59] L. Bretheau, J. I. J. Wang, R. Pisoni, K. Watanabe, T. Taniguchi and P. J. Herrero, Tunnelling spectroscopy of Andreev states in graphene, *Nat. Phys.* **13**, 756 (2017).
- [60] A. Seredinski, A. W. Draelos, E. G. Arnault, M.-T. Wei, H. Li, K. Watanabe, T. Taniguchi, F. Amet, and G. Finkelstein, Quantum Hall-based Superconducting Interference Device, *Sci. Adv.* **5**, eaaw8693 (2019).
- [61] J. Liu, J. Liu, and X. Dai, Pseudo Landau level representation of twisted bilayer graphene: Band topology and implications on the correlated insulating phase, *Phys. Rev. B* **99**, 155415 (2019).
- [62] Conventional pairing in MATBG is spatially dependent and the gap function is expressed as a matrix $\hat{\Delta}$ in Fourier space [12]. Our adiabatic approach still applies to this case, since it holds for multiband conventional SCs [29].
- [63] M. Tinkham, *Introduction to Superconductivity*, 2nd ed. (McGraw-Hill, New York, 1996).
- [64] A. S. Mayorov, D. C. Elias, I. S. Mukhin, S. V. Morozov, L. A. Ponomarenko, K. S. Novoselov, A. K. Geim, and R. V. Gorbachev, How close can one approach the Dirac point in graphene experimentally? *Nano Lett.* **12**, 4629 (2012).